

Relationship between Geomagnetic Indices (Kp, Ap) and Solar Activity (Sunspot Number)

Debasri Samanta^{1*}, Rajib Kumar Dolai²

¹Department of Physics, Vidyasagar University, Midnapore, West Bengal, India

²Department of Economics, Tamralipta Mahavidyalaya, Tamluk, West Bengal, India

Research Article

©RMC (SNSC), Tribhuvan University

ISSN: 3059-9504 (online)

DOI:<https://doi.org/10.3126/ajs.v2i1.87768>

This work is licensed under the Creative Commons CBY-NC License.

<https://creativecommons.org/licenses/by-nc/4.0/>

Article History

Received: October 16, 2025; Revised: November 14, 2025; Accepted: November 16, 2025; Published: December 25, 2025

Keywords

Sunspot Number (SSN), Kp, Ap, Time-series decomposition, Power spectral density (PSD), Cumulative distribution function (CDF).

ABSTRACT

This study examines the relationship between solar activity (Sunspot Number) (SSN) and geomagnetic indices (Kp and Ap) using time-series decomposition, distribution analysis, and correlation analysis. The results show an inverse relationship between Kp, Ap, and SSN up to 1990, followed by a strong positive correlation thereafter. Distribution analysis indicates that SSN is dominated by low-frequency components, whereas Kp and Ap capture both long-term trends and shorter-term variations, such as the ~ 27-day solar rotation cycle. Correlation analysis reveals weak overall correlations but strong trend correlations, particularly during the 12:00–15:00 UT interval for Kp and Ap with SSN.

Corresponding Author

Email: debasri94s@gmail.com (D Samanta)
Orcid: <https://orcid.org/0000-0002-1333-1189>

1. INTRODUCTION

The Sun, our nearest star, continuously emits electromagnetic radiation and charged particles into space, a process collectively referred to as solar activity. Phenomena such as sunspots, solar flares, high-speed solar wind streams, and coronal mass ejections (CMEs) influence the Earth's space environment and interact with the magnetosphere and ionosphere. When energetic solar wind plasma and interplanetary magnetic field (IMF) structures encounter Earth's geomagnetic field, they can trigger geomagnetic storms—temporary but intense disturbances in the geomagnetic field. The magnitude of these disturbances largely depends on solar wind parameters, including wind speed, density, and particularly the southward component of the IMF.

Geomagnetic activity is commonly monitored through standardized indices. The Kp index, ranging from 0 to 9, measures global geomagnetic disturbances over 3-hour intervals, whereas the Ap index represents a daily linear-scaled measure of geomagnetic activity. Solar activity is typically represented by the Sunspot Number (SSN), which varies over an approximately 11-year solar cycle. Higher SSN values correspond to solar maximum phases characterized by frequent and intense solar eruptions, while solar minimum periods reflect relatively quiet geomagnetic conditions.

The scientific literature highlights strong relationships between solar activity, solar wind conditions, and geomagnetic disturbances. Svalgaard [1] corrected the long-term Ap index to better represent geomagnetic variability, particularly during polarity intervals of the interplanetary magnetic field. Venkatesan et al. [2] identified a distinctive two-peak structure in geomagnetic activity near solar maxima. Rangarajan et al. [3] demonstrated that Kp and Ap indices exhibit seasonal and solar

cycle variations linked to solar wind dynamics, and subsequently showed that trends in Kp-based activity could be used to estimate upcoming sunspot maxima [4].

Further developments include multifractal scaling properties in geomagnetic indices reported by Yu et al. [5], and investigations by Urata et al. [6] connecting geomagnetic activity with seismic precursors, later extended by Akyol et al. [7] using ionospheric signals. Singh et al. [8] projected geomagnetic patterns for Solar Cycle 25, while Echer et al. [9] identified not only the well-known 11-year solar cycle but also a shorter 4.4-year periodicity in geomagnetic activity. Recent progress includes documentation of secular changes in the Kp index and the development of nowcast models by Matzka et al. [10], hemispheric asymmetry in solar indices reported by El-Borie et al. [11], and strong correlations between solar flare indices and geomagnetic disturbances demonstrated by Ozguc et al. [12]. Additionally, Uga et al. [13] observed significant suppression of cosmic ray intensity during geomagnetic storms, particularly at low-latitude stations, and Samanta et al. [14] applied stochastic modelling and Monte-Carlo methods in astrophysical datasets, illustrating the relevance of such methods for uncertainty estimation in space-weather analysis.

The objective of this study is to analyze the relationship between solar activity (SSN) and geomagnetic disturbances (Kp and Ap indices) using time-series analysis, distribution analysis, and correlation analysis.

2. METHODOLOGY

2.1 Data Collection

The present study utilizes complete historical time-series data, rather than sampled survey data. Therefore, population and sampling size definitions are not applicable, as the full

observational record was used to avoid any sampling bias. Daily values of the geomagnetic indices Kp and Ap were obtained from the National Centers for Environmental Information (NCEI), operated by the National Oceanic and Atmospheric Administration (NOAA). These indices are generated every three hours and subsequently aggregated to daily values. Additionally, daily Sunspot Number (SSN) data, representing solar activity levels, were sourced from the Space Weather Prediction Center (SWPC), also part of NOAA. The dataset covers the period 1932–2020, ensuring robust long-term coverage for investigating the relationship between solar activity and geomagnetic responses. Data are publicly accessible through the NOAA-NCEI geomagnetic archive (https://www.ngdc.noaa.gov/stp/geomag/kp_ap.html) and the NOAA-SWPC solar cycle database (<https://www.swpc.noaa.gov/products/solar-cycle-progression>).

2.2 Seasonal-Trend Decomposition Method

To extract long-term patterns and recurring seasonal behavior from the time-series data, we applied the Seasonal-Trend decomposition using Loess (STL) [15] technique. STL is a robust, non-parametric framework that decomposes a time series into three components: a trend component T_t capturing long-term changes, a seasonal component S_t representing periodic fluctuations, and a residual component R_t that accounts for random irregular variations. Mathematically, the series Y_t at time t is represented as

$$Y_t = T_t + S_t + R_t \quad \dots \quad (1)$$

Each component is estimated independently, allowing the decomposition to adapt flexibly to non-linear structures present in geomagnetic and solar data.

2.3 Distribution Method

To study the frequency structure and statistical distribution of geomagnetic indices (Kp, Ap) and solar activity (SSN), we employed Power Spectral Density (PSD) and Probability Density Function (PDF) analysis. Daily Kp and Ap values were computed as the mean of eight 3-hour measurements recorded each day. The PSD quantifies how variance (power) is distributed across frequency components, enabling identification of dominant periodicities. PSD was estimated using Welch's method, where the signal is segmented, windowed, and Fourier-transformed. For a segment index k and frequency f , the spectral estimate is

$$P_{xx}(f) = \frac{1}{N} \sum_{k=1}^K |X_k(f)|^2 \quad \dots \quad (2)$$

where:

- $P_{xx}(f)$ is the estimated power at frequency f ,
- N is the number of segments into which the time series is divided,
- K is the total number of segments,
- $X_k(f)$ is the Fourier transform of the k -th segment of the time series.

The PDF describes the probability of the time-series variable taking a particular value. For observations X_i and bin width Δx , the PDF is defined as

$$PDF(x) = \frac{1}{N\Delta x} \sum_{i=1}^N \delta(x - X_i) \quad \dots \quad (3)$$

where:

- $PDF(x)$ is the probability density at value x ,
- N is the total number of observations,
- Δx is the bin width,
- X_i represents each individual observation in the time series,
- $\delta(x - X_i)$ is an indicator function that counts the occurrences of values in the range of bin x .

Additionally, the Cumulative Distribution Function (CDF) of the PSD evaluates the cumulative contribution of frequencies to total power. For frequencies $f' \leq f$, the CDF is expressed as

$$CDF_{PSD}(f) = \frac{\sum_{f' \leq f} P_{xx}(f')}{\sum_{f'} P_{xx}(f')} \quad \dots \quad (4)$$

which enables quantification of low- versus high-frequency dominance in geomagnetic variability.

2.4 Correlation Method

To examine the statistical association between geomagnetic activity (Kp and Ap) and solar activity (SSN), we employed the Pearson correlation coefficient, which measures the linear dependence between two variables. For paired observations X_i (e.g., daily Kp or Ap) and Y_i (daily SSN), the coefficient r is given by

$$r = \frac{\sum_{i=1}^n (X_i - \bar{X})(Y_i - \bar{Y})}{\sqrt{\sum_{i=1}^n (X_i - \bar{X})^2} \sqrt{\sum_{i=1}^n (Y_i - \bar{Y})^2}} \quad \dots \quad (5)$$

where \bar{X} and \bar{Y} represent the mean values of the respective series and n is the number of paired observations. The value of r ranges between -1 and $+1$, indicating negative, positive, or no linear correlation.

3. RESULTS AND DISCUSSION

The analysis begins by examining the long-term variability of solar activity and its connection with geomagnetic indices. As shown in Fig. 1, the Sunspot Number (SSN) exhibits a strong linkage with the Kp and Ap indices. Peaks in SSN, corresponding to solar maxima, generally coincide with elevated values of Kp and Ap, confirming that periods of intense solar activity are accompanied by enhanced geomagnetic disturbances. This suggests that increases in SSN, reflecting higher sunspot activity, are associated with corresponding rises in Kp and Ap due to the intensified impact of solar forcing on Earth's magnetosphere. The characteristic \sim 11-year solar cycle observed in SSN is also mirrored in the variations of Kp and Ap, indicating a recurring pattern of enhanced geomagnetic activity that aligns with solar cycle phases. To explore these relationships in greater detail, time-series decomposition, distributional characteristics, and correlation analyses were conducted.

3.1 Time-Series Decomposition Analysis

The decomposition of the data provides insights into long-term trends, seasonal cycles, and irregular variations of SSN, Kp, and Ap indices.

The long-term trends of the Kp and Ap geomagnetic indices, alongside SSN, show distinct behaviors across the observation period. While Kp and Ap display pronounced fluctuations with peaks and troughs reflecting changing levels of geomagnetic activity, they also reveal a gradual downward trend toward the end of the series. In contrast, SSN exhibits a steady overall decline in solar activity. A closer look at the SSN trend reveals three distinct segments: (i) a sharp decline until 1960, (ii) a moderate decline between 1960 and 1990, and (iii) a rapid decline after 1990. When compared with the geomagnetic indices, contrasting patterns emerge in the earlier periods. During the first segment, while SSN declines sharply, Kp and Ap increase significantly. Between 1960 and 1990, Kp and Ap continue to rise, though at a slower rate, whereas SSN declines moderately. In the final period (1990–2020), all three indices exhibit a synchronized downward trend, indicating strong alignment between solar and geomagnetic activity in recent decades (Fig. 2).

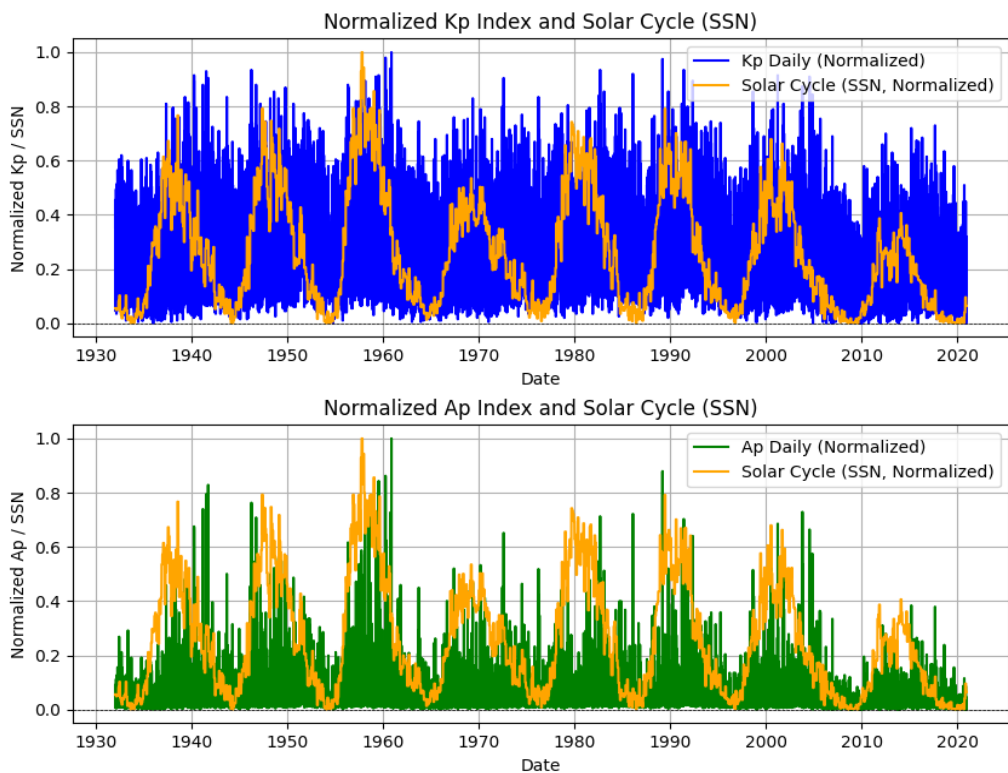


Fig. 1: Normalized Sunspot Number (SSN) and Geomagnetic Indices (Kp and Ap) [Source: Designed by the authors (Using python)]

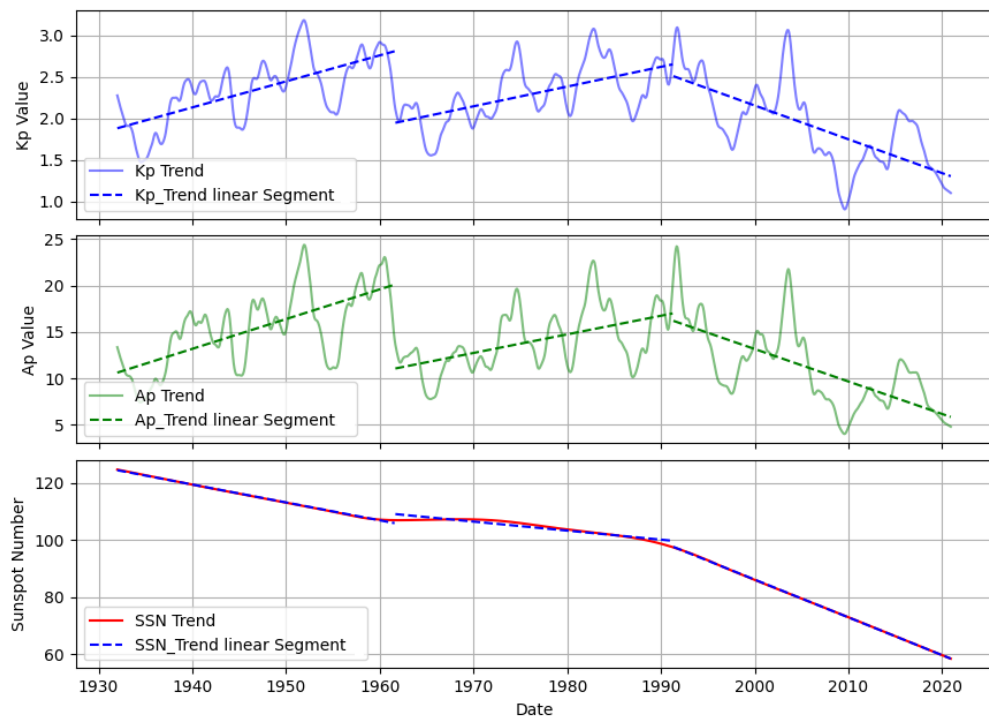


Fig. 2: Trends Components in Kp, Ap, and SSN [Source: Designed by the authors (Using python)]

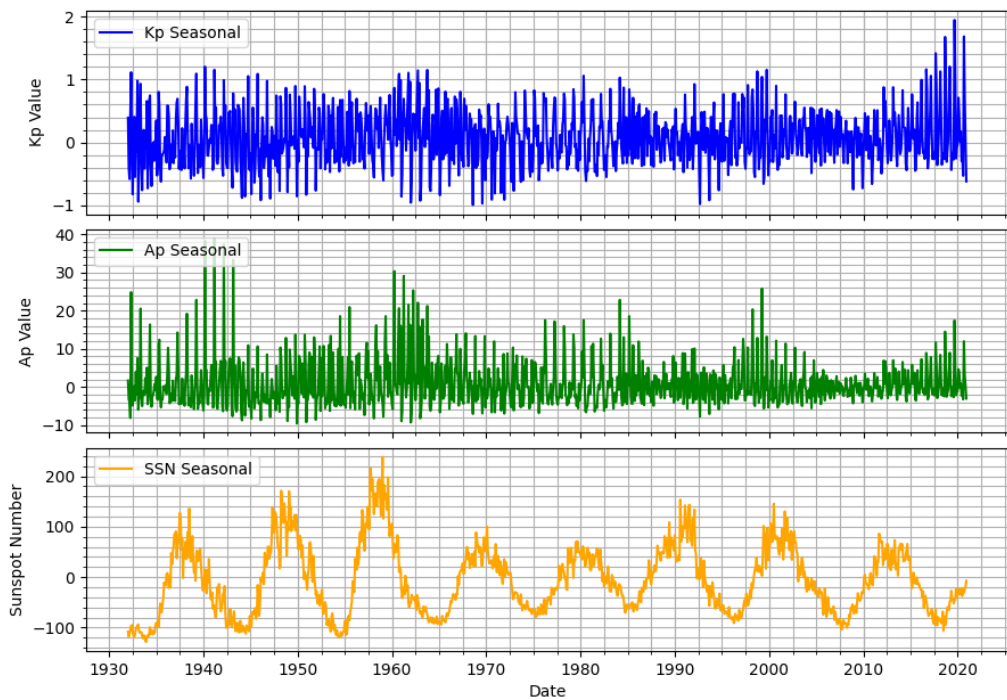


Fig. 3: Seasonal Components in Kp, Ap, and SSN [Source: Designed by the authors (Using python)]

The seasonal decomposition highlights the cyclical behavior of solar and geomagnetic indices. The Kp index exhibits consistent semi-annual oscillations, reflecting Earth's orbital position relative to solar wind input. The Ap index also displays a seasonal pattern, but with greater amplitude, indicating heightened sensitivity to intense geomagnetic disturbances, likely driven by strong solar wind streams or coronal mass ejections. SSN, in turn,

mirrors the ~11-year solar cycle, with peaks corresponding to solar maxima and troughs to minima (Fig. 3). These seasonal components demonstrate the close coupling between solar cycles and geomagnetic responses, with notable impacts observed during the 1960s, 1990s, and 2000s, when solar maxima significantly amplified geomagnetic activity (Fig. 4).

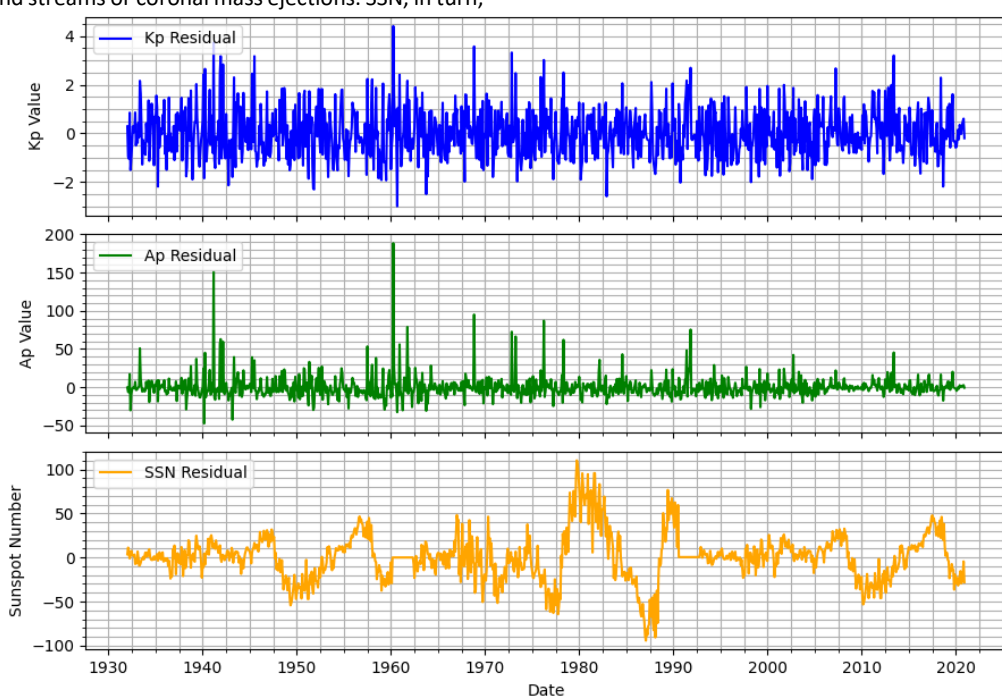


Fig. 4: Residual Components of Kp, Ap, and SSN Indices After Decomposition [Source: Designed by the authors (Using python)]

The residuals capture irregular, non-periodic fluctuations beyond the trend and seasonal components. Kp residuals remain relatively stable, with small random deviations, suggesting that the decomposition captures most of its variability. By contrast, Ap residuals display sharp spikes, reflecting episodic geomagnetic disturbances such as geomagnetic storms triggered

by solar eruptions. SSN residuals show irregular anomalies and bursts, pointing to deviations from the expected solar cycle and potential disruptions in typical solar activity patterns. These irregularities underline the complex and sometimes unpredictable nature of solar-terrestrial interactions.

3.2 Distribution Analysis

In the distribution analysis of the Kp and Ap indices, as well as SSN, the patterns of geomagnetic and solar activity are examined. Fig. 5 shows the Power Spectral Density (PSD) and Probability Density Function (PDF) for these indices, highlighting their temporal dynamics and distributions. The PSD plots for Kp and Ap reveal prominent peaks at frequencies around 0.02–0.1 cycles per day, corresponding to periodic phenomena such as the ~27-day solar rotation and transient geomagnetic disturbances. In contrast, the SSN PSD is dominated by low frequencies,

reflecting the influence of long-term solar cycles, such as the 11-year solar cycle. The ~27-day solar rotation period is calculated from the PSD as the reciprocal of the frequency ($p = 1/f$) where a peak is observed, typically around 0.037 cycles per day, yielding a period of approximately 27 days. This reflects the synodic rotation of the Sun, where active regions like coronal holes and sunspots reappear periodically, influencing solar wind patterns and driving geomagnetic activity. The broader peaks in the PSD of Ap and Kp imply cumulative effects from prolonged solar influences, such as recurrent geomagnetic storms or extended solar wind interactions.

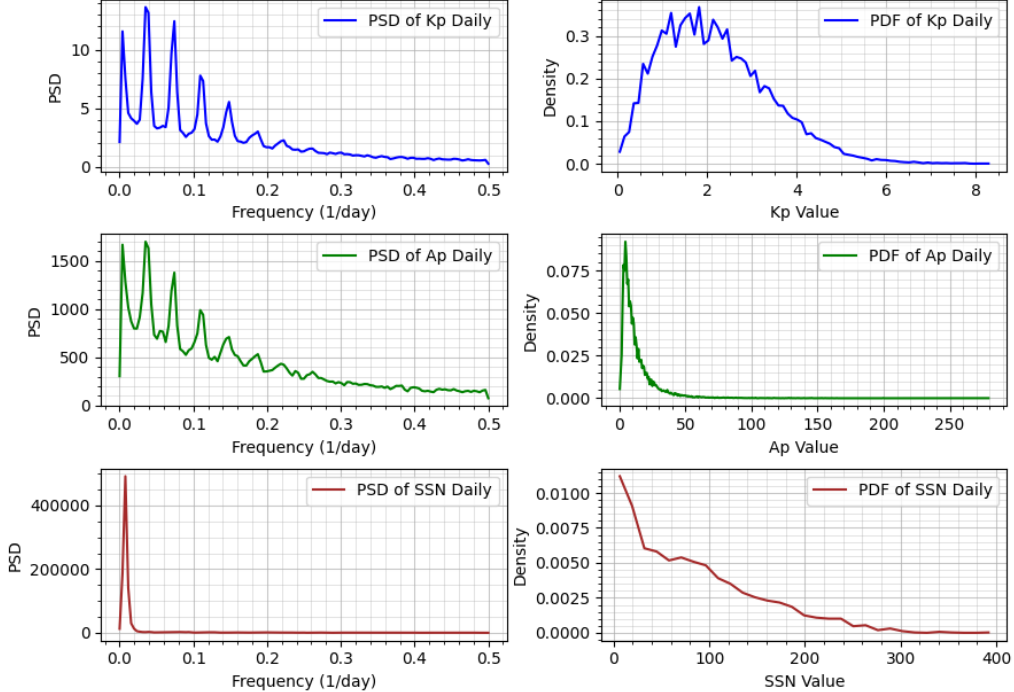


Fig. 5: Power Spectral Density and Probability Density Functions of Kp, Ap, and SSN Indices [Source: Designed by the authors (Using python)]

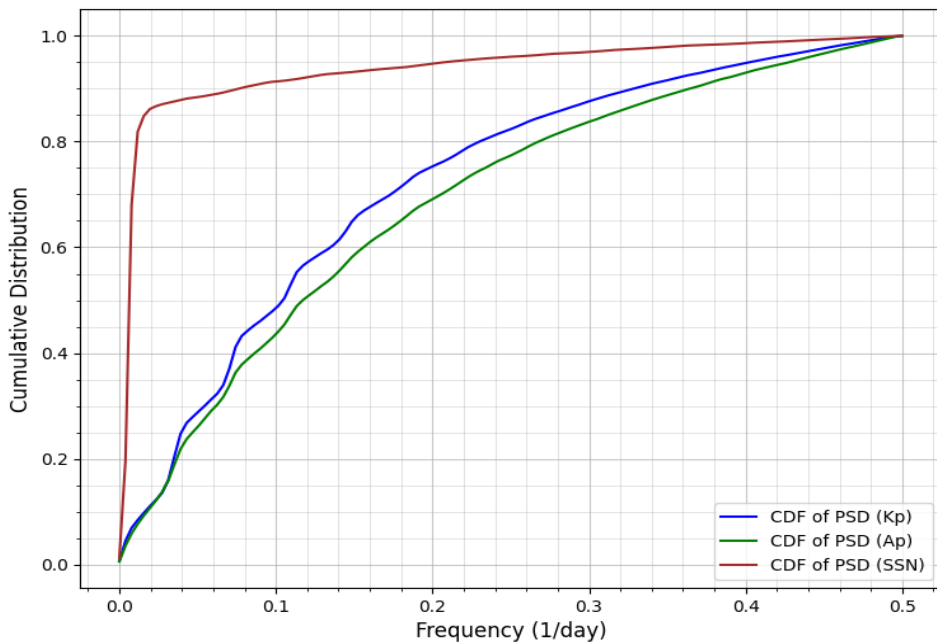


Fig. 6: Cumulative Distribution of PSD for Kp, Ap, and SSN Indices [Source: Designed by the authors (Using python)]

The PDFs indicate that Kp and Ap values are concentrated at lower magnitudes, reflecting the predominance of moderate

geomagnetic activity. Their longer tails capture the occurrence of infrequent but extreme events, particularly for Ap, which reflects

planetary-scale geomagnetic disturbances. The density of Kp values is most prominent in the range of 0.99–2.45, whereas Ap shows stronger concentration between 3.16 and 4.57. In contrast, the SSN PDF displays a gradual decline, with most values clustered at lower sunspot counts, consistent with the prevalence of relatively quiet solar periods. These results suggest that while SSN primarily governs long-term geomagnetic trends, Kp and Ap are strongly shaped by short-term solar and interplanetary dynamics, with Ap being especially sensitive to extreme geomagnetic events.

The cumulative distribution function (CDF) of the power spectral density (PSD) for the Kp, Ap, and SSN indices reveals distinct differences in the frequency characteristics of solar and geomagnetic activity. For the Sunspot Number (SSN), the CDF shows a sharp rise at very low frequencies, confirming that most of its spectral power is concentrated in this range. This reflects the dominance of long-term periodicity, particularly the 11-year solar cycle, and indicates that sunspot activity evolves gradually under the influence of slow, decadal-scale solar magnetic processes with limited higher-frequency contributions. In contrast, the CDFs of Kp and Ap increase more gradually across a wider frequency band, demonstrating that geomagnetic activity is driven not only by the solar cycle but also by short-term variations. These include the quasi-27-day solar rotation, seasonal modulations, and transient solar disturbances such as coronal mass ejections (CMEs) and high-speed solar wind streams, which induce rapid fluctuations in Earth's magnetosphere. Furthermore, the Ap CDF is slightly less steep at low frequencies compared to Kp, suggesting that Ap captures a broader spectrum of geomagnetic disturbances, including cumulative or prolonged activity, whereas Kp is more sensitive to intermittent variations (Fig. 6).

Correlation Analysis

To better understand the relationship between solar activity and geomagnetic disturbances, correlations were computed between the Sunspot Number (SSN) and the geomagnetic indices Kp and Ap, considering their overall, trend, seasonal, and

residual components (Table 1). The overall correlations are relatively weak, with Kp–SSN at 0.1948 and Ap–SSN at 0.1564, suggesting only a mild positive association between geomagnetic activity and solar activity when all components are combined. The trend component exhibits the strongest correlations, with Kp–SSN at 0.6303 and Ap–SSN at 0.5951, underscoring the dominant role of long-term solar cycles in shaping geomagnetic variations. By contrast, the seasonal correlations are negligible—0.0282 for Kp and 0.0273 for Ap—indicating that short-term periodicities in geomagnetic indices are not strongly aligned with the seasonal variation of sunspot activity. Residual correlations are also minimal, with Kp–SSN at 0.0246 and Ap–SSN at -0.0086, showing little to no relationship between high-frequency fluctuations in solar and geomagnetic activity (Fig. 5). Overall, these findings confirm that the long-term solar trend exerts a significant influence on geomagnetic indices, while seasonal and short-term fluctuations remain largely independent of sunspot variations.

Table 1: Correlation Analysis of Kp and Ap Indices (Average of 3-hour Intervals) with Sunspot Number (SSN).

	Overall	Trend	Seasonal	Residual
Correlation between Kp and SSN	0.1948	0.6303	0.0282	0.0246
Correlation between Ap and SSN	0.1564	0.5951	0.0273	-0.0086

[Source: By the authors (Using Excel &Python)]

To further investigate how solar activity relates to short-term geomagnetic variations, correlations were computed between the Sunspot Number (SSN) and 3-hour interval values of the geomagnetic indices Kp and Ap across four components: overall, trend, seasonal, and residual (Table 2). The overall correlation is relatively strong between Kp 5_15h and SSN, with a value of 0.1946.

Table 2: Correlation Analysis of 3-hour interval values of Kp and Ap with Sunspot Number (SSN).

Correlation	Overall	Trend	Seasonal	Residual
Correlation between Kp1_3h and SSN	0.1302	0.4283	-0.0724	0.0207
Correlation between Kp2_6h and SSN	0.1430	0.4564	-0.0598	0.0173
Correlation between Kp3_9h and SSN	0.1679	0.491	0.0114	0.0195
Correlation between Kp4_12h and SSN	0.1867	0.5198	-0.0788	0.0247
Correlation between Kp5_15h and SSN	0.1946	0.5579	0.018	0.0277
Correlation between Kp6_18h and SSN	0.1750	0.5279	-0.0925	0.0219
Correlation between Kp7_21h and SSN	0.1540	0.4807	-0.0594	0.0167
Correlation between Kp8_24h and SSN	0.1381	0.4457	-0.0176	0.0183
Correlation between Ap1_3h and SSN	0.1050	0.4777	-0.0657	0.0188
Correlation between Ap2_6h and SSN	0.1133	0.5095	0.01	0.0162
Correlation between Ap3_9h and SSN	0.1231	0.5228	0.0718	0.0206
Correlation between Ap4_12h and SSN	0.1311	0.5245	0.013	0.0255
Correlation between Ap5_15h and SSN	0.1451	0.5932	0.0931	0.0308
Correlation between Ap6_18h and SSN	0.1328	0.5635	-0.0015	0.0269
Correlation between Ap7_21h and SSN	0.1190	0.5259	-0.0432	0.0187
Correlation between Ap8_24h and SSN	0.1098	0.4942	-0.0421	0.0186

Source: By the authors (Using Excel & Python)

More pronounced relationships emerge in the trend component, where correlations range from 0.4283 to 0.5579 for Kp and from 0.4777 to 0.5932 for Ap, highlighting the dominant influence of long-term solar activity patterns on geomagnetic indices even at shorter temporal resolutions. Notably, the highest trend correlation occurs during the 12:00–15:00 UT interval for both Kp5_15h and Ap5_15h with SSN. This elevated correlation likely reflects the combined effects of enhanced dayside geomagnetic activity and the persistence of solar cycle-driven responses reinforced by cumulative solar–terrestrial interactions during this time window. By contrast, seasonal correlations are weak—often close to or below zero—suggesting minimal periodic alignment between geomagnetic fluctuations and SSN at 3-hour scales. Residual correlations are negligible across all intervals, indicating that high-frequency variations in geomagnetic indices bear little connection to sunspot activity. An important pattern, however, is that correlations, particularly in the trend component, tend to strengthen with longer averaging intervals for both Kp and Ap, implying that the influence of solar activity becomes clearer when aggregated over time.

4. CONCLUSIONS

This study examined the relationship between solar and geomagnetic activity using time-series decomposition, distribution analysis, and correlation analysis. The decomposition highlights how the linkage between sunspot activity and geomagnetic indices evolves over time: until 1990, Kp and Ap trends show an inverse relationship with SSN, while after 1990 a strong positive association emerges. Seasonal components capture periodic signatures, such as the semi-annual variations in Kp and Ap and the ~11-year solar cycle in SSN. Residuals reveal irregular, short-term disturbances, with Ap displaying sharp spikes tied to transient geomagnetic storms and SSN showing bursts of irregular solar activity.

The spectral and probability distribution analyses reveal distinct temporal and amplitude characteristics. SSN is dominated by low-frequency components, reflecting the long-term solar cycle, whereas Kp and Ap span broader frequency ranges, capturing both long-term cycles and shorter-term variations such as the ~27-day solar rotation. Probability distributions confirm that moderate geomagnetic activity is most frequent, while Ap is more responsive to extreme planetary-scale disturbances compared to Kp.

Correlation analysis offers a quantitative perspective on the solar–geomagnetic relationship across components and timescales. While overall associations are positive but weak, trend components display the strongest correlations, emphasizing the dominant role of long-term solar cycles in driving geomagnetic variability. The highest trend correlations occur during the 12:00–15:00 UT interval for both Kp5_15h and Ap5_15h with SSN, likely reflecting enhanced dayside activity and cumulative solar–terrestrial interactions. Seasonal correlations are weak, underscoring limited solar–geomagnetic periodic alignment, and residual correlations are negligible or slightly negative, pointing to the independence of high-frequency geomagnetic fluctuations from solar activity.

AUTHOR CONTRIBUTIONS

All the authors contributed equally.

CONFLICT OF INTEREST

The authors declare no competing interests with respect to the publication of this manuscript.

ACKNOWLEDGMENTS

We sincerely thank Dr. Anurag Sahay (NIT Patna) and Dr. Bappasona Kar (Panskura Banamali College) for their valuable guidance and insights, which greatly enhanced this study. We are also grateful to Soumen Khatua (NIT Patna) for his constant support and encouragement.

FUNDING

This research received no specific grant from any funding agency in the public, commercial, or not-for-profit sectors.

REFERENCES

- [1] L. Svalgaard, Recalibration of Bartels' geomagnetic activity indices Kp and ap to include UT variations, *Journal of Geophysical Research*, **81** (1976) 5182-5188. <https://doi.org/10.1029/JA081i028p05182>
- [2] D. Venkatesan, A.G. Ananth, H. Graumann, S. Pillai, Relationship between solar and geomagnetic activity, *Journal of Geophysical Research: Space Physics*, **96** (1991) 9811-9813. <https://doi.org/10.1029/90JA02322>
- [3] G.K. Rangarajan, T. Lyemori, Time variations of geomagnetic activity indices Kp and Ap: an update, *Annales Geophysicae*, **15** (1997) 1271-1290. <https://doi.org/10.1007/s00585-997-1271-z>
- [4] G.K. Rangarajan, L.M. Barreto, Use of Kp index of geomagnetic activity in the forecast of solar activity, *Earth, Planets and Space*, **51** (1999) 363-372. <https://doi.org/10.1186/BF03352240>
- [5] Z-G. Yu, V. Anh, R. Eastes, Underlying scaling relationships between solar activity and geomagnetic activity revealed by multifractal analyses, *Journal of Geophysical Research, Space Physics*, **119** (2014) 7577-7586. <https://doi.org/10.1002/2014JA019893>
- [6] N. Urata, G. Duma, F. Freund, Geomagnetic Kp index and earthquakes, *Open Journal of Earthquake Research*, **7** (2018) 39-52. <https://doi.org/10.4236/ojer.2018.71003>
- [7] A.A. Akyol, O. Arikan, F. Arikan, A machine learning-based detection of earthquake precursors using ionospheric data, *Radio Science*, **55** (2020) 1-21. <https://doi.org/10.1029/2019RS006931>
- [8] P.R. Singh, A.I.S. Farid, A.K. Singh, T.K. Pant, A.A. Aly, Predicting the maximum sunspot number and geomagnetic indices for solar cycle 25, *Astrophysics and Space Science*, **366** (2021) 48. <https://doi.org/10.1007/s10509-021-03953-3>
- [9] E. Echer, L.E.A. Vieira, N.R. Rigozo, M.P. Souza, D.J.R. Nordemann, A study of solar-geomagnetic indices correlation, 7th Int. Congress of the Brazilian Geophysical Society, (2001) cp-217. https://mtcm16.sid.inpe.br/attachment.cgi/sid.inpe.br/marciana/2005/01.24.15.56/doc/SBGF2001-%20Analyses_
- [10] J. Matzka, C. Stolle, Y. Yamazaki, O. Bronkalla, A. Morschhauser, The geomagnetic Kp index and derived indices of geomagnetic activity, *Space Weather*, **19** (2021) e2020SW002641. <https://doi.org/10.1029/2020SW002641>
- [11] M.A. El-Borie, A.M. El-Taher, A.A. Thabet, S.F. Ibrahim, A.A. Bishara, North–South asymmetry of some solar

parameters during solar cycles 18–24, *Chinese Journal of Physics*, **72** (2021) 1-17.
<https://doi.org/10.1016/j.cjph.2021.02.007>

[12] A. Ozguc, A. Kilcik, V. Yurchyshyn, Temporal and periodic variations of the solar flare index during the last four solar cycles and association with geomagnetic parameters, *Solar Physics*, **297** (2022) 112.
<https://par.nsf.gov/servlets/purl/10427551>

[13] C.I. Uga, S.P. Gautam, E.B. Seba, Cross-correlation analysis of cosmic ray intensity with interplanetary and geomagnetic parameters, *Cosmic Research*, **62** (2024) 34-41. <https://doi.org/10.1134/S0010952523600075>

[14] D. Samanta, R.K. Dolai, Stochastic modeling of compact binary coalescences for gravitational wave analysis, *International Astronomy and Astrophysics Research Journal*, **7** (2025) 57-67.
<https://doi.org/10.9734/iaarj/2025/v7i1116>

[15] R.B. Cleveland, STL: A seasonal-trend decomposition procedure based on LOESS, *Journal of Official Statistics*, **6** (1990) 3-73. <https://www.wessa.net/download/stl.pdf>